

Analysis of Daxis and Qaxis Inductance Estimation of Interior Permanent Magnet Synchronous Motor

Gang-Hyeon Jang, Sung-Won Seo, Chang-Woo Kim, Kyung-Hun Shin, Jeong-In Lee, Tae-Kyoung Bang, Ick-Jae Yoon, Jang-Young Choi

Abstract Background/Objectives: In this study, the d and qaxis inductance values of interior permanent magnet (PM) motors are analyzed accurately using by finite element analysis.

Methods/Statistical analysis: Herein, based on an element analysis method, no-load and load conditions of a PM motor are investigated. The inductance values of the d and qaxis were analyzed using the magnetic flux estimation method.

Findings: The inductance of the interior PM motor is analyzed and the torque value is calculated based on the inductance. The calculated results were compared and analyzed with the experimental results.

Improvements/Applications: The inductance map can be derived by using the method proposed in this research, and the d and qaxis inductance values, which are difficult to actually measure, can be accurately analyzed.

Keywords: Interior PM synchronous motor (IPMSM), Inductance analysis, Torque calculation

I. INTRODUCTION

Since the late 1900s, the use of interior PM synchronous motors in place of direct current (DC) motors has been on the rise across the industry, owing to its high output and high-efficiency characteristics. Because the permanent magnet is embedded in the inner barriers of the IPMSM rotor, it is possible to prevent the PM from scattering by the centrifugal force arising from the high mechanical strength in high-speed operations [1-2]. Because the magnetic torque and the reluctance torque are structurally generated simultaneously, a high torque can be produced. In addition, it is possible to perform a wide range of operations, including flux weakening control, by using a salient pole. The steady-state performance analysis and high-performance control of an interior permanent magnet synchronous motor are largely dependent on the accurate measurement and estimation of the motor parameters. To apply the maximum torque (MT) per ampere control, it is necessary to know the value of the stator resistance, the inductance, and the motor constant, such as the flux linkage formed by the permanent magnet. It is essential for motor control that the phase

inductance is expressed in a time constant that synchronizes with the driving frequency of the motor because of the structural feature that causes the phase inductance to vary with the PM position. Therefore, the phase inductance is analyzed by dividing the d and qaxis equivalently, and this value is used for motor control [3-5].

II. ANALYSIS OF THE IPMSM

The essential parameters of the interior PM synchronous motor are the flux linkage of PMs and the inductance of the d and qaxis. A careful approach is required because it affects the saturation of the d and qaxis [6-7]. In general, various methods can be used to obtain the d and qaxis inductance, which is an important parameter of the motor, and they can be roughly divided into the finite element (FE) method and the measurement method by experiment. For the finite element method, the inductance value can be estimated by considering the saturation of the motor. Finite element estimation can also be used to predict the performance at the design stage. To use the FE method, it is essential to know the structure of the motor and the dimensions of each part. The estimated values need to be verified using empirically measured values. In this research, the d and qaxis inductances, which are important parameters of the interior PM synchronous motor, are analyzed by the FE method according to the current magnitude and beta angle, and the analysis results are verified through experiments. Table 1 shows the motor specifications. The rotor has a PM with six poles embedded in it, and the armature winding made of copper is wound around the stator iron core having nine slots by concentric winding. Figure 1 shows the shape and winding pattern of the interior PM motor. Table 2 shows the winding specification of the motor.

Revised Manuscript Received on May 22, 2019.

Gang-Hyeon Jang, Sung-Won Seo, Chang-Woo Kim, Kyung-Hun Shin, Jeong-In Lee, Tae-Kyoung Bang, Ick-Jae Yoon, Jang-Young Choi, Department Electrical Engineering, Chungnam National University, Yuseong-gu, Daejeon, 34134, Korea

gh.jang@cnu.ac.kr¹, dd1059@cnu.ac.kr², demona@cnu.ac.kr³, sinkyunghun@cnu.ac.kr⁴, lji477@cnu.ac.kr⁵, bangtk77@cnu.ac.kr⁶, ijyoon@cnu.ac.kr⁷, choi_jy@cnu.ac.kr⁸



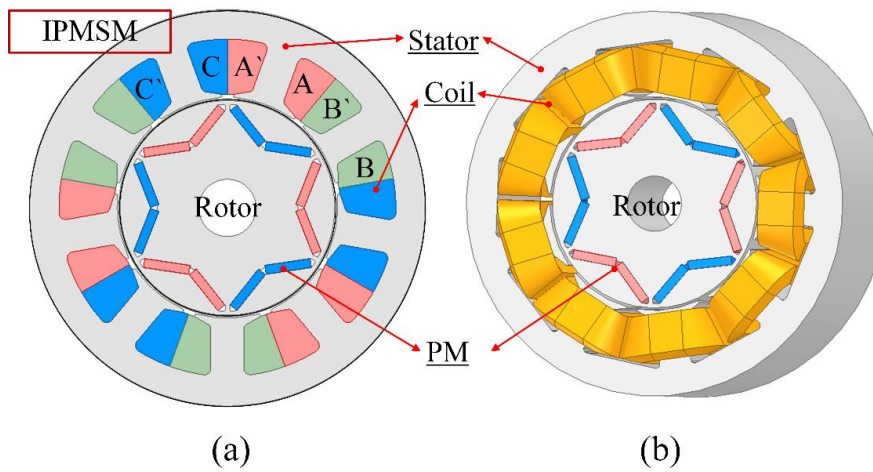


Figure 1. (a) Analysis model, (b) 3D FEM model

Table 1. Specification of the IPMSM

Parameter	Spec.	Parameter	Spec.
Torque	2 ~ 4 Nm	Outer diameter	90 mm
Pole number	6	Stack length	40 mm
Slot number	9	Core material	35PN440
Speed	15 ~ 120Hz	PM material	NdFeB

Table 2. Winding specifications of the IPMSM

Parameters	Value	Unit
Slot area	180	mm ²
Turn per slot	152	
Number of parallel branch	1	
Wire diameter	0.75	Mm
Strands	1	
Temperature	75	°C
Resistance	1.49	Ω
Fill factor	37.3	%

2.1. No load analysis results of IPMSM

When the permanent magnet rotor is rotated (no load condition) after modeling by using the finite element analysis program, the flux linkage, back electromotive force, and cogging torque are analyzed. The cogging torque is caused by the change of the reluctance to the circumferential change by the magnetic field generated in the field and the stator

tooth-slot structure. The cogging torque implies a torque in a radial direction, in which a non-uniform torque is to be moved to a position where magnetic energy is minimum. The back electromotive force refers to the voltage generated when the magnetic flux is linked to the armature winding by the rotation of the permanent magnet rotor. The back electromotive force is determined by equation (1).

$$E_{max} = N_m k_d k_p B_r L_{stk} N_{turns} \omega_n \quad (1)$$

Where N_m is the number of poles, k_d is the distribution coefficient, k_p is the cutoff factor, B_r is the maximum value of the airgap magnetic flux density, L_{stk} is the axial stack length of the stator core, N_{turns} is the number of turns, and ω_n is the angular rotation speed.

The analysis of the cogging torque can be confirmed by rotating the motor in a no-load state, and as a result of the resulting torque value. The waveform and size of the cogging torque of the motor are shown in Figure 2 (a). The value of the cogging torque is 39.8 mNm.

Figure 2 (b) shows the results of the no-load EMF (Electro Motive Force) analysis of the PM motor. The analysis condition is 1000 rpm (50 Hz), and the value of 45.4 Vrms of line back-EMF is confirmed. The back electromotive force constant can be calculated using Equation (2).

$$K_e = \max \left(\frac{V_{emf}}{\omega_e} \right) \quad (2)$$

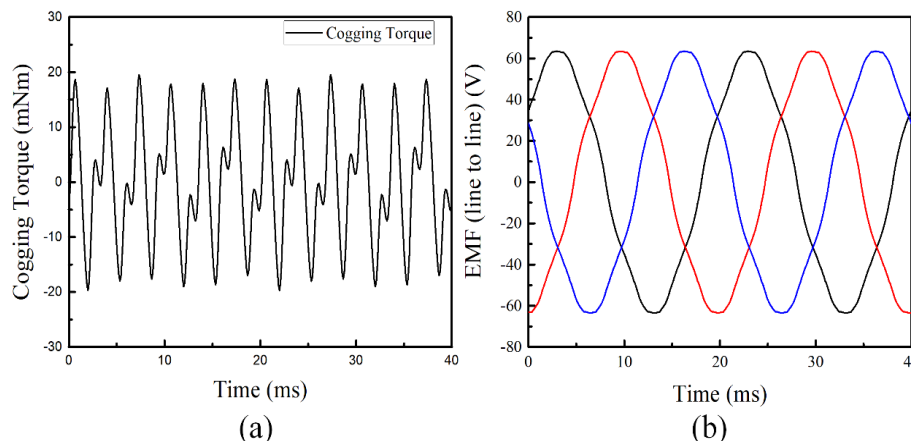


Figure 2. A no-load analysis result of IPMSM: (a) cogging torque (b) EMF

2.2. Load analysis results of IPMSM

In this paper, a FE analysis program was used to verify the load characteristics of PM motors. The torque generated by applying the current to the model was confirmed, and the reliability of the analysis was confirmed through experiments.

Figure 3 (a) shows torque analysis results when a phase current of 4 Arms is applied at 800 rpm. Torque values were found to be 2.71 Nm on average. Torque ripple is calculated

to be 11.61%. Figure 3 (b) shows the result of back EMF analysis of the motor under load. The line back-EMF was confirmed to be 40.1 Vrms. This allows the voltage limit to be predicted. Figure 4(a) shows torque analysis results when a phase current of 3.5 Arms is applied at 1400 rpm. The torque value was confirmed to be 2.4 Nm on average. Torque ripple was calculated to be 12.22%. Fig. 4 (b) shows the results of the analysis of the line-to-line back electromotive force occurring when the phase current of 3.5 Arms at 1400 rpm is applied. It can be confirmed that a back electromotive force of 68.8 Vrms is generated.

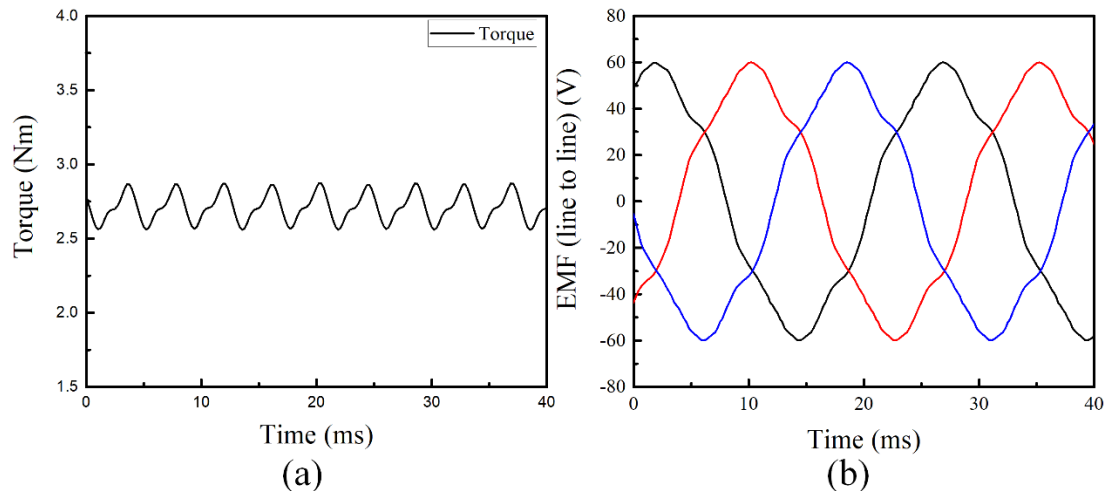


Figure 3. Load analysis result of IPMSM at 800rpm condition: (a) Out torque (b) L_L EMF

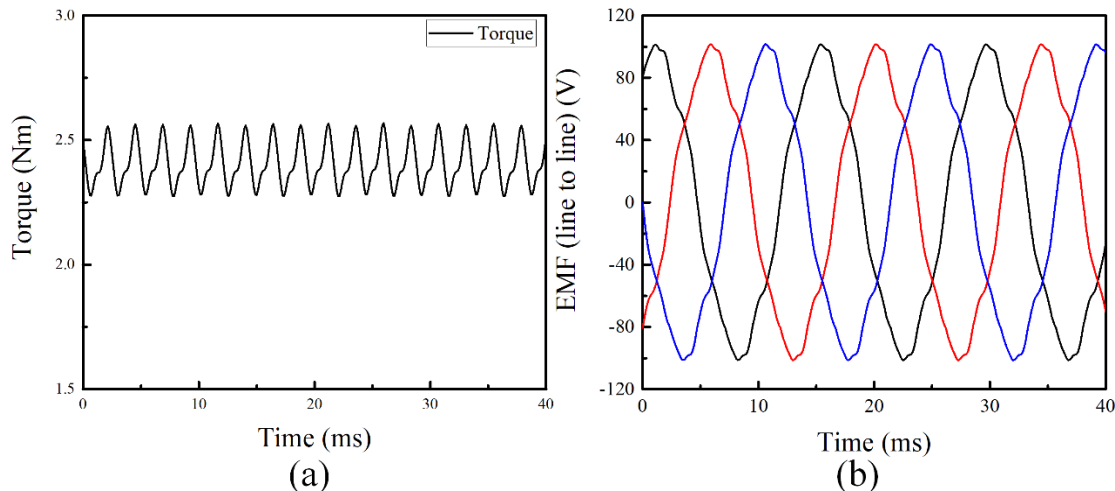


Figure 4. Load analysis result of IPMSM at 1400rpm condition: (a) Out torque (b) L_L EMF

III. INDUCTANCE ESTIMATION OF IPMSM

We used the flux vector method to extract the inductance using the finite element method. Figure 5 shows the vector diagram of the IPMSM.

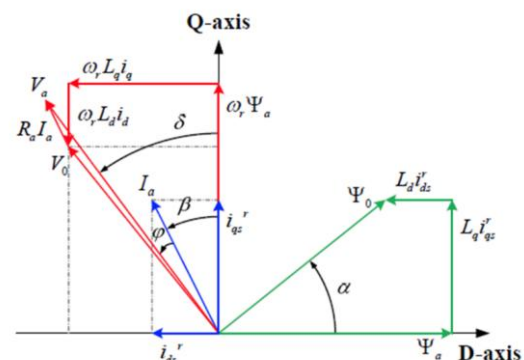


Figure 5. The vector diagram of the IPMSM for

calculated daxis and qaxis inductance.

In Fig. 5, the daxis and qaxis current can be expressed by the following equation (3). The effective value of the fundamental wave component in the flux linkage at the time of loading is expressed by equation (4). The rms value of the fundamental wave component in the no-load condition is expressed by Eq. (5). Next, the values of daxis and qaxis inductance can be calculated by the equations (6, 7), where α represents the phase difference of flux linkage between load and no-load conditions [8-10].

$$\begin{bmatrix} i_d \\ i_q \end{bmatrix} = \begin{bmatrix} -i_a \sin \beta \\ i_a \cos \beta \end{bmatrix} \quad (3)$$

$$\psi_a = \sqrt{3} \psi_{ua} \quad (4)$$

$$\psi_o = \sqrt{3} \psi_{uo} \quad (5)$$

$$L_q = \frac{\psi_o \sin \alpha}{i_q} \quad (6)$$

$$L_d = \frac{\psi_o \cos \alpha - \psi_a}{i_d} \quad (7)$$

torque of the permanent magnet motor can be expressed by the following equation (8). In this case, equation (9) denotes the magnetic torque, and the reference numeral (10) denotes the reluctance torque.

$$T = P_n \{ \psi_a i_a \cos \beta + 0.5 (L_q - L_d) i_a^2 \sin 2\beta \} \quad (8)$$

$$T_e = P_n (\psi_a i_a \cos \beta) \quad (9)$$

$$T_r = P_n \{ 0.5 (L_q - L_d) i_a^2 \sin 2\beta \} \quad (10)$$

3.1. Inductance analysis according to the current phase angle

The following figure shows the result of the daxis inductance analysis according to the current magnitude and beta angle. The current beta angle (30–60°) is shown according to the current magnitude. The daxis inductance generally tends to decrease as the current magnitude increases. However, when the beta angle is generated, as shown in Figure 6, the daxis inductance tends to increase and decrease to a constant current.

Figure 7 shows the torque analysis using finite element analysis, the comparison of the torque values through experiments, the torque calculated based on the inductance and current magnitude, the phase angle, the linkage flux, and the experiment. It is confirmed that the results of the calculated torque values are in well agreement with the experimental results of the FEM method. It is considered that the extraction of the d-axis and q-axis inductance values used in the electromagnetic torque modification is relatively accurate.

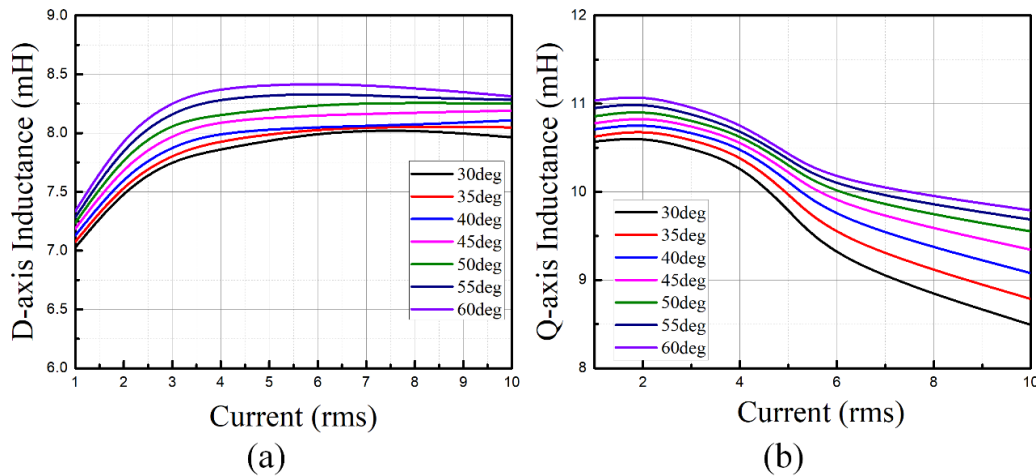


Figure 6. Analysis result of daxis and qaxis inductance of Interior PM Synchronous Motor according to the current magnitude and current beta angle.

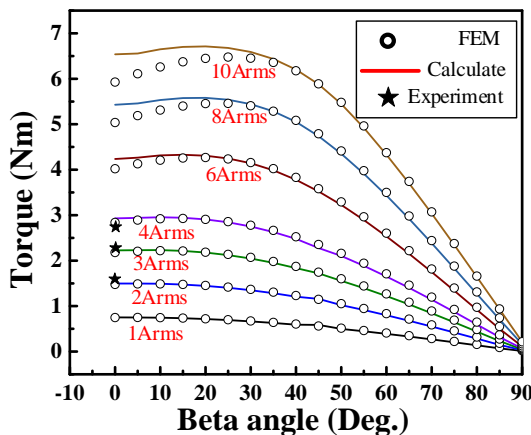


Figure 7. Comparison of torque measurement, analysis, calculated results according to current magnitude and current angle.

IV. EXPERIMENT AND ANALYSIS RESULTS

The back-to-back set is composed of two identical motors, a torque sensor, and a speed sensor for the load test when the permanent magnet motor is in the no-load condition. Fig 8(a) shows the experimental setup for evaluating the IPMSM. The oscilloscope is configured to measure the back-EMF and load-to-line voltage, phase current, torque, and speed when no load is applied. In order to confirm the reliability of the analysis, the back EMF

was measured and compared through experiments. Fig. 8(b) shows the experimental result of back EMF in the load condition. As a result, it was confirmed that the magnitude and waveform of the back EMF were in good agreement, and the reliability of the modeling and analysis results of the motor was confirmed. Table 3 shows the experimental results of the permanent magnet motor under load. When the same current is applied, a similar torque value is output in the experiment and analysis. Therefore, the results of the finite element analysis are considered reliable.

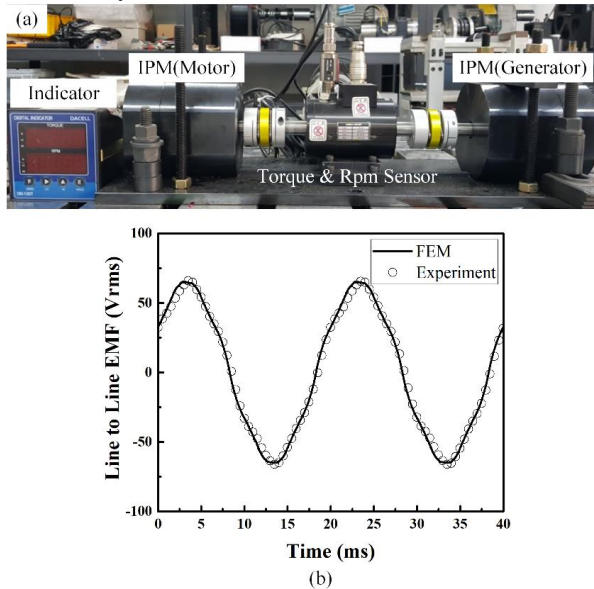


Figure 8. (a) Back-to-Back system for performance evaluation of IPMSM (b) measurement and analysis results of motor back EMF.

Table 3. Permanent magnet motor load test results

Speed	Parameters	Analysis	Experiment
800 Rpm	Torque	2.71 Nm	2.73 Nm
	Phase Current	4A _{rms}	4A _{rms}
1400 Rpm	Torque	2.4 Nm	2.36 Nm
	Phase Current	3.5A _{rms}	3.5A _{rms}

V. CONCLUSION

This paper deals with the inductance calculate of the d and qaxis of an IPMSM. After modeling the permanent magnet motor, the flux value was obtained through no-load analysis and load analysis. The inductance equation was derived using the vector diagram of the model, and the torque value at the load was calculated using the analyzed inductance value. Using the experimental set, the performance of the motor with no load and with load was confirmed. The calculated torque values were verified by comparison with experimental results. Using the analyze method presented in this study, the inductance of the PM motor can be accurately analyzed.

ACKNOWLEDGMENT

This work was supported by the Korea Institute of Energy Technology Evaluation and Planning (KETEP) Grants No. 20172010105590 funded by the Korean Ministry of Trade, Industry (MOTIE).

This work was supported by the Basic Research Laboratory (BRL) of the National Research Foundation (NRF-2017R1A4A1015744) funded by the Korean government.

REFERENCES

1. W. Huang, Y. Zhang, X. Zhang, and G. Sun. Accurate Torque Control of Interior Permanent Magnet Synchronous Machine. *IEEE Trans. Energy Convers.* 2012; 29(1).
2. J. Y. Choi, Y. S. Park, and S. M. Jang. Experimental Verification and Electromagnetic Analysis for Performance of Interior PM Motor According to Slot/Pole Number Combination. *IEEE Trans. Magn.* 2012; 48(2).
3. K. D. Lee, H. W. Lee, J. Lee, and W. H. Kim. Analysis of Motor Performance According to the Inductance Design of IPMSM. *IEEE Trans. Magn.* 2015; 51(3).
4. A. Wang, Y. Jia, and W. L. Soong. Comparative of five topologies for an interior permanent-magnet machine for a hybrid electric vehicle. *IEEE Trans. Magn.* 2011; 47(10).
5. Mohammad SedighToulabi, John Salmon, and Andrew M. Knight. Design, Control, and Experimental Test of an Open-Winding IPM Synchronous Motor. *IEEE Trans. Ind. Elec.* 2017; 64(4).
6. W. H. Kim, M. J. Kim, K. D. Lee, J. J. Lee, J. H. Han, T. C. Jeong, S. Y. Cho, and J. Lee. Inductance Calculation in IPMSM Considering Magnetic Saturation. *IEEE Trans. Magn.* 2014; 50(1).
7. C. Lai, G. Feng, K. Mukherjee, V. Loukanov, C. Kar. Torque Ripple Modeling and Minimization for Interior PMSM Considering Magnetic Saturation. *IEEE Trans. Ind. Elec.* 2018;33(3).
8. Y. S. Chen, Z. Q. Zhu, and D. Howe. Calculation of d- and q- Axis Inductance on PM Brushless ac Machines Accounting for Skew. *IEEE Trans. Magn.* 2005;41(10).
9. K. J. Meessen, P. Thelin, J. Soulard, and E. A. Lomonova. Inductance Calculation of Permanent-Magnet Synchronous Machines Including Flux Change and Self- and Cross-Saturations. *IEEE Trans. Magn.* 2008; 44(10).
10. R. Dutta and M. F. Rahman. A comparative analysis of two testmethods of measuring d- and q-axes inductances of interior permanent-magnet machine. *IEEE Trans. Magn.* 2006; 42(11).